

Physico–mathematical model of the voltage–current characteristics of light-emitting diodes with quantum wells based on the Sah–Noyce–Shockley recombination mechanism

Fedor I. Manyakhin¹, Dmitry O. Varlamov¹, Vladimir P. Krylov², Lyudmila O. Morketsova³, Arkady A. Skvortsov^{1,†}, and Vladimir K. Nikolaev¹

¹Dynamics, Strength of Machines and Resistance of Materials, Moscow Polytechnic University, Russia

²Biomedical and Electronic Means and Technologies, Vladimir State University, Russia

³Computer-Aided Design and Engineering, National University of Science and Technology "MISiS", Russia

Abstract: Herein, a physical and mathematical model of the voltage–current characteristics of a p–n heterostructure with quantum wells (QWs) is prepared using the Sah–Noyce–Shockley (SNS) recombination mechanism to show the SNS recombination rate of the correction function of the distribution of QWs in the space charge region of diode configuration. A comparison of the model voltage–current characteristics (VCCs) with the experimental ones reveals their adequacy. The technological parameters of the structure of the VCC model are determined experimentally using a nondestructive capacitive approach for determining the impurity distribution profile in the active region of the diode structure with a profile depth resolution of up to 10 Å. The correction function in the expression of the recombination rate shows the possibility of determining the derivative of the VCCs of structures with QWs with a nonideality factor of up to 4.

Key words: light-emitting diodes with quantum wells; voltage–current relation; nonideality factor; recombination mechanism; Sah–Noyce–Shockley model

Citation: F I Manyakhin, D O Varlamov, V P Krylov, L O Morketsova, A A Skvortsov, and V K Nikolaev, Physico–mathematical model of the voltage–current characteristics of light-emitting diodes with quantum wells based on the Sah–Noyce–Shockley recombination mechanism[J]. *J. Semicond.*, 2024, 45(8), 082102. <https://doi.org/10.1088/1674-4926/23120044>

1. Introduction

Classical models of current–voltage characteristics of semiconductor diodes. There are two main physical and mathematical models of the dependence of current through a p–n structure on the bias voltage applied to it, namely, the Shockley model^[1] and the Sah–Noyce–Shockley (SNS) model^[2], which are utilized for modeling solar cells^[3] and photodetectors^[4, 5], modeling the instability behavior of thin-film devices^[6], describing the behavior of voltage–current characteristics (VCCs) of semiconductor diodes, and analyzing the physical processes that form these characteristics.

The Shockley model of the so-called ideal diode is expressed as Refs. [1, 7]:

$$J_d = q \left(\frac{D_n}{L_n N_a} + \frac{D_p}{L_p N_p} \right) n_i^2 \left[\exp\left(\frac{qU}{kT}\right) - 1 \right] = J_0 \left[\exp\left(\frac{qU}{kT}\right) - 1 \right], \quad (1)$$

where q refers to the elementary charge, n_i refers to intrinsic concentration of charge carriers, D_n and D_p represent the diffusion coefficients of electrons and holes, respectively, L_n and L_p represent the diffusion lengths of electrons and holes, respectively, N_a and N_d represent the concentrations of acceptors and donors in the p- and n-regions of an abrupt p–n junc-

tion, respectively, U refers to the bias voltage at the potential barrier of the p–n junction (space-charge region (SCR)), k is the Boltzmann constant, and T refers to the absolute temperature of the p–n junction, $J_0 = q \left(\frac{D_n}{L_n N_a} + \frac{D_p}{L_p N_p} \right) n_i^2$ refers to the saturation current in the diffusion model.

The Shockley model is based on the idea that under forward bias U , the potential barrier of the p–n junction φ_k decreases by value qU and diffusion flows of electrons from the n-region to the p-region and holes from the p-region to the n-region enter its adjacent regions. As minority carriers in adjacent regions, they impair their electrical neutrality. To maintain the electrical neutrality of the n- and p-regions, the main charge carriers enter them through the contact terminals during Maxwellian relaxation.

Injected holes and electrons, when diffusing, recombine and produce the so-called diffusion current. Thus, this model is also called the diffusion model. The fundamental aspect is that this model does not consider recombination in the space charge region (SCR) of the p–n junction, and the current is generated only by charge carriers that have overcome the potential barrier.

The exponent in Eq. (1) is a consequence of the Boltzmann energy distribution of charge carriers in the quasineutral p and n regions.

The SNS model, unlike the Shockley model, considers the recombination current in the SCR p–n junction through local deep energy levels in the band gap. Moreover, because charge carriers with energy less than the potential barrier

Correspondence to: A A Skvortsov, skvortsova2009@hotmail.com

Received 26 DECEMBER 2023; Revised 1 MAY 2024.

©2024 Chinese Institute of Electronics

height are involved in the recombination process in the SCR, the rate of their recombination under certain conditions can be higher than that of charge carriers that have overcome the potential barrier. Consequently, the SNS model is called the generation–recombination model (the reverse bias mode will not be considered; therefore, we will use the name "recombination model").

Consequently, the SNS model is called a generation–recombination model (herein, we did not consider the reverse bias mode; instead, we used the term recombination model).

The SNS model for direct current is expressed mathematically as following equation^[8]:

$$J_r = \frac{1}{2} \sigma N_t W V_T n_i \exp\left(\frac{qU}{2kT}\right) = J_s \exp\left(\frac{qU}{2kT}\right), \quad (2)$$

where q refers to the elementary charge, σ indicates the cross section for the capture of charge carriers by local recombination centers, N_t refers to the concentration of recombination centers in the SCR, W refers to the width of the space charge region, V_T refers to the thermal velocity of charge carriers, n_i refers to the intrinsic concentration of charge carriers, and $J_s = \frac{1}{2} \sigma N_t W V_T n_i$ indicates the saturation current.

Coefficient "2" in the Eq. (2) exponent is usually called the nonideality factor (in some works, the ideality factor) of the VCC. In this work we will use the former name. The physical meaning of this coefficient is as follows. In accordance with the SNS theory, with a uniform distribution of the concentration of recombination centers in the SCR and the location of their energy levels near the middle of the band gap, the maximum recombination rate, given that the grip section of electrons and holes is the same at the centers, is achieved for charge carriers with an energy equal to half the contact potential after deduction of bias voltage $E_{max} = (\varphi_k - qU)/2$. Here, it is necessary to emphasize the assumption^[8] of a uniform distribution of a relatively high concentration of recombination centers in the SCR, creating a quasicontinuous energy level of trapped charge carriers with an equal probability across the entire width of the SCR. This assumption enables us to obtain a simple equation (Eq. (5)) for the direct current (Eq.(2)).

However, experimental studies of the defect distribution near the metallurgical boundary of p–n structures reveal that it is far from uniform^[9, 10]. In this case, the recombination rate may depend on the coordinate in the SCR differently than in the case of a uniform distribution of point defects, i.e. it may be determined by some distribution function of recombination centers.

For many years, authors studying VCCs explained the deviation of the nonideality factor using $n = 2$ by competition in the total current of diffusion and recombination currents or tunneling^[8]:

$$J = J_0 \exp\left(\frac{qU}{kT}\right) + J_s \exp\left(\frac{qU}{2kT}\right). \quad (3)$$

Previous studies did not consider that point and extended defects can occur at the metallurgical boundary during formation of a p–n junction, and that their concentration exponentially decreases with distance from it^[9, 10]. Consequently, maximum recombination rate will not occur in the

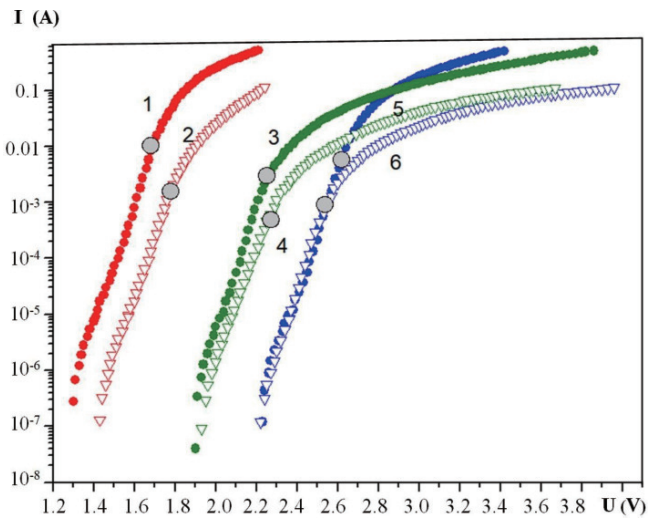


Fig. 1. (Colour online) Voltage–current characteristics of light-emitting diodes with different energies of emitted quanta and power consumption (different current densities). Gray circles represent the currents where the voltage–current characteristics (VCCs) start to deviate from the exponential dependence of current on voltage.

middle of the SCR (i.e., the charge carrier energy corresponding to half of the contact potential minus the mixing voltage potential $(\varphi_k - qU)$).

The use of VCC models has become more complicated with the advent of light-emitting diode (LED) structures with quantum wells^[1, 2, 5–7]. Difficulties have arisen in explaining the VCC behavior within a large range of changes in direct current, within which the VCC derivative changes its value many times. Moreover, VCC derivative values can exceed the theoretical one by several times^[11, 12]. Interpretations of this phenomenon are varied^[13, 14]. In some cases, it is associated with the mechanism of recharging deep levels in the SCR band gap^[15–17]. The following may be another cause of change in VCC derivative with change in bias voltage: (a) change in injection level^[18], (b) influence of contact resistance, and (c) base region of the crystals.

A previous study^[11] demonstrated that LED structures with quantum wells can be represented as p–n junctions with extended recombination centers in the form of layers of quantum wells with a capture cross section close to unity. These centers are separated by layers with no recombination, which are called separation barriers.

Thus, to mathematically describe the VCC model of structures with quantum wells, the SNS model can be applied with an additional distribution function of quantum wells as recombination centers located on gap H as the width of the quantum wells, separated by the gap of the width of the separation barriers, where there are no recombination centers.

An equally important characteristic of the VCCs of p–n structures based on high-bandgap semiconductors, such as GaN, AlInGaP, and SiC, is the sharp deviation of the dependence of current on voltage (towards an increase in voltage by the amount indicated by U_i in Fig. 1) from the exponential form at current densities above 1–10 A/cm². This deviation starts at almost identical current densities for light-emitting diodes with different energies of emitted light quanta (Fig. 1). The gray circles in the figure refer to the current values where the VCC deviation from the exponential depen-

dence begins. In this case, the crystal areas of low-power and high-power light-emitting diodes differ by approximately seven times.

An analysis of the proportions of voltages U_i and U_b in this section shows that the series resistance $R_b = U_b/I$ in it depends on the current and has a maximum value at a certain value.

Studies on the degradation of light-emitting diodes^[19] revealed that luminous flux decreases most intensely during long-term current flow, specifically in regimes where the VCCs deviate from the exponential.

This work aimed to develop, based on the SNS model, a modernized model of the VCCs of LED structures with quantum wells and to determine its adequacy with experimental VCCs.

The study objectives include: (1) obtaining experimental VCCs of light-emitting diodes in the current range of up to 10^{-11} A (current densities up to 10^{-8} A/cm²) and their derivatives to measure the performance of the modernized SNS model; (2) establishing the relation between the change in the VCC derivative in semilogarithmic coordinates and the parameters of the quantum-dimensional structure; and (3) identifying the mechanism of the VCC deviation from the exponential dependence in the region having a current density above 1–10 A/cm².

Low-power LEDs of the GNL type were used as model objects, in particular, as an example, green LEDs GNL-3014PGC.

2. Results and discussion

Upgraded Sah–Noyce–Shockley VCC model for light-emitting diode structures with quantum wells. The primary parameters of the model of light-emitting diode structures with QWs for the VCCs include: (1) the degree of doping, N_a and N_d of the p- and n-regions, respectively, (2) the number of QWs and their coordinates μ , (3) the width of QWs H , (4) the carrier capture cross section with QWs σ , and (5) the band gap, E_G and E_{QW} , of the barrier region and QWs, respectively. The physical parameters of the semiconductors are taken elsewhere^[20, 21].

The proposed mathematical model of the VCCs of LEDs with quantum wells is obtained from the original equation for the distribution of the recombination rate along the coordinate in the SCR of the p–n junction^[2]:

$$R(x) = \frac{V_T \sigma_n \sigma_p N_t [n(x)p(x) - n_1^2]}{\sigma_n [n(x) + n_1] + \sigma_p [p(x) + p_1]}, \quad (4)$$

where V_T is the thermal velocity of charge carriers, σ_n and σ_p are the electron and hole capture cross sections averaged over all states at a given center, N_t is the concentration of capture centers, $n(x)$ and $p(x)$ are the concentrations of electrons and holes along the x coordinate in the SCR of the p–n junction, and n_1 and p_1 are concentrations of electrons and holes corresponding to the energy position of the level of capture centers in the band gap:

$$n_1 = N_C \exp\left(-\frac{E_{tn}}{kT}\right), \quad p_1 = N_V \exp\left(-\frac{E_{tp}}{kT}\right), \quad (5)$$

where N_C and N_V are the densities of states in the conduc-

tion and valence bands, respectively, and E_{tn} and E_{tp} are the energy positions of capture levels in the band gap for electrons and holes, respectively.

In this study, we assume that the LED p–n structure is sharply asymmetrical, that both regions are evenly doped, and that the n region is doped more than the p region $N_d \gg N_a$. Consequently, the conduction band potential in the SCR of lightly doped region without bias voltage changes as per the following quadratic law:

$$\varphi_n = \frac{qN_a}{2\varepsilon\varepsilon_0} [(W(0)^2 - (W(0) - x)^2)] = \varphi_k \left[\frac{2x}{W(0)} - \frac{x^2}{W(0)^2} \right]. \quad (6)$$

However, it changes as follows when applying forward bias voltage:

$$\varphi_n(x) = (\varphi_k - qU) \left[\frac{2x}{W(U)} - \frac{x^2}{W(U)^2} \right], \quad (7)$$

for valence band top,

$$\varphi_p(x) = (\varphi_k - qU) \left[1 - \left(\frac{2x}{W(U)} - \frac{x^2}{W(U)^2} \right) \right]. \quad (8)$$

In these dependences, φ_k represents contact potential, $W(0)$ represents the width of the SCR in the absence of bias voltage, and $W(U)$ represents the width of the SCR with applied bias voltage U . The following equations express distribution of concentration of electrons and holes in the SCR along the x coordinate:

$$n(x, U) = N_d \exp(-\varphi_k + qU) \left[\frac{2x}{W(U)} - \frac{x^2}{W(U)^2} \right], \quad (9)$$

$$p(x, U) = N_a \exp(-\varphi_k + qU) \left[1 - \left(\frac{2x}{W(U)} - \frac{x^2}{W(U)^2} \right) \right]. \quad (10)$$

We modeled the SCR potential via linear approximation as follows:

$$n(x, U) = N_d \exp(\varphi_k - qU) \left[\frac{x}{W(U)} \right], \\ p(x, U) = N_a \exp(\varphi_k - qU) \left[1 - \frac{x}{W(U)} \right], \quad (11)$$

which showed that it does not introduce considerable distortions into the VCC form. However, this study used the quadratic dependence of potential on the coordinate.

We present a single quantum well as an extended, two-level capture center with its own concentration $N_t = 1$ with the same electron and hole capture cross-section σ . The electron capture level is the top of the QW valence band, and the level of holes is the bottom of the QW conduction band. Charge carriers recombine through these centers. Calculation results show that n_1 and p_1 in the denominator of Eq. (9) can be neglected in the temperature range of 0–50 °C at a forward bias voltage of more than 0.35 V.

Furthermore, radiative recombination of charge carriers is known to occur in quantum wells according to the

zone–zone mechanism; however, it does not occur in the region of separation barriers. Therefore, we assume that the probabilities of recombination via the SNS mechanism of electrons and holes in a quantum well are 1 and 0, respectively, in the region of the separation barriers. We express this probability by the function $f(x) = 0$ with $x < \mu \pm H/2 < x$, $f(x) = 1$ with $x = \mu \pm H/2$. Here, μ represents the coordinate of the middle of the quantum well, measured from the metallurgical boundary (in the heavily doped layer). Notably, there are no point defects in the SCRs, and there is no Auger recombination in the quantum wells.

$$R(x, U) = \frac{f(x) \sigma N_t V_T \beta}{N_d \exp \left\{ \left(\frac{-\varphi_k + qU}{kT} \right) \left[\frac{2x}{W(U)} - \frac{x^2}{W(U)^2} \right] \right\} + N_a \exp \left\{ (-\varphi_k + qU) \left[1 - \left(\frac{2x}{W(U)} - \frac{x^2}{W(U)^2} \right) \right] \right\}} \\ \times \left\{ N_d N_a \exp \left\{ \left(\frac{-\varphi_k + qU}{kT} \right) \left[\frac{2x}{W(U)} - \frac{x^2}{W(U)^2} \right] \right\} \exp \left\{ (-\varphi_k + qU) \left[1 - \left(\frac{2x}{W(U)} - \frac{x^2}{W(U)^2} \right) \right] \right\} - n_i^2 \right\}, \quad (12)$$

considering that $\frac{N_d N_a}{n_i^2} = \exp \left(\frac{\varphi_k}{kT} \right)$, we perform substitutions in the numerator and introduce the designation $r = N_d/N_a$; we

$$R(x, U) = \frac{f(x) \sigma N_t V_T N_d \left[\exp \left(\frac{-\varphi_k + qU}{kT} \right) - 1 \right]}{r \exp \left\{ \left(\frac{-\varphi_k + qU}{kT} \right) \left[\frac{2x}{W(U)} - \frac{x^2}{W(U)^2} \right] \right\} + \exp \left\{ (-\varphi_k + qU) \left[1 - \left(\frac{2x}{W(U)} - \frac{x^2}{W(U)^2} \right) \right] \right\}}. \quad (13)$$

In this form of expression of recombination rate, a heavily doped layer of a sharply asymmetric p–n structure represents an injector with a concentration of charge carriers at the bottom of the conduction band N_d , which flow at a thermal velocity to the potential barrier (i.e., SCR). Charge carriers with energy corresponding to quantum well energy posi-

In addition, at the bottom of the quantum well for electrons (for holes, this is the valence band top of the QW), the concentration of injected charge carriers is β times greater than that at the edge of the separation barrier: $\beta = \exp \left(\frac{E_g - E_{QW}}{2kT} \right)$. We assumed that the energy depth of the quantum wells is the same for electrons and holes, and that the energy at the bottom (top) of the quantum wells does not depend on x .

Eq. (4) takes the following form under the abovementioned assumptions:

$$obtain the following equation upon removing the common factor from the denominator:$$

$$R(x, U) = \frac{f(x) \sigma N_t V_T N_d \left[\exp \left(\frac{-\varphi_k + qU}{kT} \right) - 1 \right]}{r \exp \left\{ \left(\frac{-\varphi_k + qU}{kT} \right) \left[\frac{2x}{W(U)} - \frac{x^2}{W(U)^2} \right] \right\} + \exp \left\{ (-\varphi_k + qU) \left[1 - \left(\frac{2x}{W(U)} - \frac{x^2}{W(U)^2} \right) \right] \right\}}. \quad (13)$$

In this form of expression of recombination rate, a heavily doped layer of a sharply asymmetric p–n structure represents an injector with a concentration of charge carriers at the bottom of the conduction band N_d , which flow at a thermal velocity to the potential barrier (i.e., SCR). Charge carriers with energy corresponding to quantum well energy posi-

$$tion enter it and recombine.$$

For a structure with one quantum well ($N_t = 1$), the dependence of current density on voltage at $qU > 14 kT$ (for $T = 300$ K, the condition $U > 0.35$ V was previously accepted) being unity in the numerator can be neglected, following which the current density is expressed as:

$$J(U) = J_{0r} \int_0^{W(U)} \frac{f(x) \exp \left(\frac{-\varphi_k + qU}{kT} \right)}{r \exp \left\{ \left(\frac{-\varphi_k + qU}{kT} \right) \left[\frac{2x}{W(U)} - \frac{x^2}{W(U)^2} \right] \right\} + \exp \left\{ (-\varphi_k + qU) \left[1 - \left(\frac{2x}{W(U)} - \frac{x^2}{W(U)^2} \right) \right] \right\}} dx, \quad (14)$$

where $J_{0r} = q\sigma N_t \beta V_T N_d$. The capture cross-sectional area is equal to $\sigma = 1$ because (i) the area of quantum wells is equal to that of the p–n structure and (ii) all nonequilibrium carriers entering it recombine according to the conditions of the model.

The integral in Eq. (14) cannot be expressed in the form of a familiar exponent with a constant preexponential factor

$$J(U) = J_{0r} \int_0^{W(U)} \frac{F(x) \exp \left(\frac{-\varphi_k + qU}{kT} \right)}{r \exp \left\{ \left(\frac{-\varphi_k + qU}{kT} \right) \left[\frac{2x}{W(U)} - \frac{x^2}{W(U)^2} \right] \right\} + \exp \left\{ (-\varphi_k + qU) \left[1 - \left(\frac{2x}{W(U)} - \frac{x^2}{W(U)^2} \right) \right] \right\}} dx = J_{0r} \text{Ex}(U), \quad (15)$$

where $\text{Ex}(U)$ denotes the integral in this equation.

We review another option for obtaining a VCC model. We consider that the quantum well width is sufficiently small,

because this is a more complex function than a simple exponent. Moreover, for one quantum well, as will be shown later, the exponential dependence of current on voltage is violated within a certain range of bias voltages.

The recombination probability function $F(x)$ will be equal to the sum $f(x)$ for a structure with multiple quantum wells. One has

i.e., 3–4 nm, to consider the type of distribution $R(x, U)$ in it to be trapezoidal. Accordingly, current in one quantum well can be calculated via some approximation as:

$$J_1(U) = J_{0r} \frac{H \exp \left(\frac{-\varphi_k + qU}{kT} \right)}{r \exp \left\{ \left(\frac{-\varphi_k + qU}{kT} \right) \left[\frac{2\mu}{W(U)} - \frac{\mu^2}{W(U)^2} \right] \right\} + \exp \left\{ (-\varphi_k + qU) \left[1 - \left(\frac{2\mu}{W(U)} - \frac{\mu^2}{W(U)^2} \right) \right] \right\}}. \quad (16)$$

Table 1. Initial parameters of the VCC model of the GNL-3014PGC light-emitting diode with one, two, and five quantum wells.

$N_d (10^{19} \text{ cm}^{-3})$	$N_a (10^{17} \text{ cm}^{-3})$	$N_{ai} (10^{16} \text{ cm}^{-3})$	$\mu_1 (10^{-6} \text{ cm})$	$\mu_2 (10^{-6} \text{ cm})$	$\mu_3 (10^{-6} \text{ cm})$	$\mu_4 (10^{-6} \text{ cm})$	$\mu_5 (10^{-6} \text{ cm})$	$H (10^{-7} \text{ cm})$
2	2	4	4.14	—	—	—	—	4.0
2	2	4	2.1	4.5	6.9	—	—	4.0
2	2	3	1.14	2.64	4.14	5.64	7.14	4.0

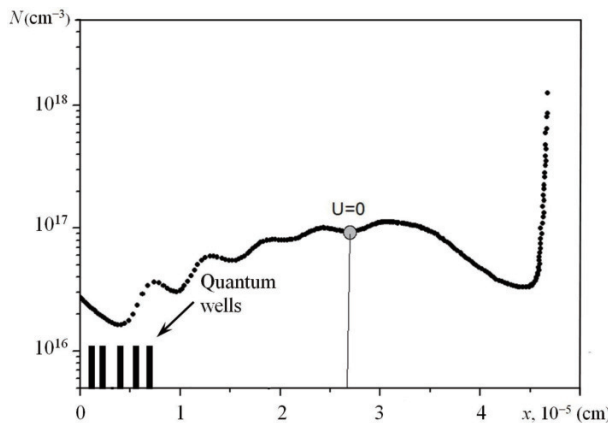


Fig. 2. Distribution of impurity concentration in the region showing changes in the space charge of the GNL-3014PGC light-emitting diode. The gray circle indicates the position of the SCR edge in the absence of bias voltage.

Because the recombination flows of quantum wells are parallel, the total current of an LED with multiple quantum wells will be equal to the sum of currents of all quantum wells. If the fraction in Eq. (16) is denoted by $Y_1(U)$ to shorten the equation, then the equation for the VCC in this case takes the form

$$J_{0QW} = qH\sigma N_t \beta V_t N_d \sum_n Y_1(U). \quad (17)$$

This approach to the VCC model of an LED structure with QWs allows for us to state that the VCC equation of p–n structures with multiple QWs does not represent a traditionally written exponential with a bias-voltage-dependent nonideality factor in the indicator but is a sum of exponential dependencies. This results in the experimentally observed multiple changes in the VCC derivative. Moreover, as will be shown later, this is ascribed to change in positions of maximum recombination rate and SCR edge relative to location of quantum wells.

We experimentally measured the impurity distribution profile in the active region of the GNL-3014PGC (Fig. 2) green light-emitting diode structure using the non-destructive method described by Shockley *et al.*[22] and Kudryashov *et al.*[23] as well as using a designed and created computerized installation controlled by an ATmega8 microcontroller. The profile parameters were recorded in a file with the *.txt extension and further processed and analyzed (Fig. 2). The profile depth resolution was $1 \times 10^{-7} \text{ cm}$ (approximately three atomic layers at a concentration of charged centers of $1 \times 10^{17} \text{ cm}^{-3}$).

Note that several works regarding the distribution of the concentration of charge centers in the region of QWs revealed the presence of a layer up to $4 \times 10^{-5} \text{ cm}$ wide near the metallurgical boundary of the p–n junction, with an impurity concentration of the order of 1×10^{16} – $1 \times 10^{17} \text{ cm}^{-3}$,

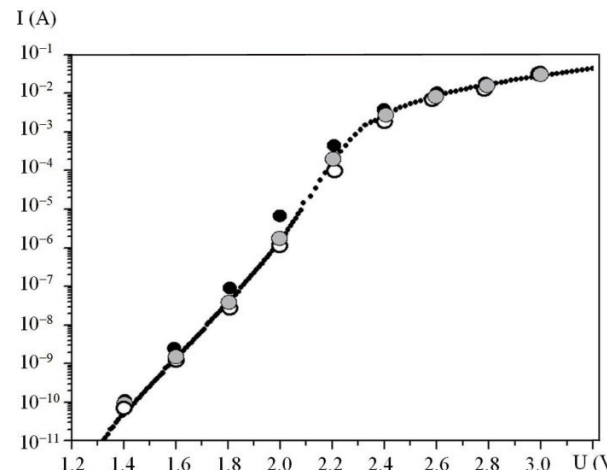


Fig. 3. Volt–ampere characteristics of the GNL-3014PGC light-emitting diode. White dots refer to the VCC coordinates for a structure with one quantum well (QW), gray dots refer to the coordinates of the model VCC with three QWs, and black dots refer to the coordinates with five QWs. The calculation parameters are taken from Table 1.

where the SCR propagates. The bars in Fig. 2 indicate conventionally the location of the QW.

Based on the distribution profile of the electrically active impurity in the active layer, the following should be noted. The active layer is nonuniformly doped. The region adjacent to the metallurgical boundary, a few hundredths of a micrometer wide, is alloyed to a level of approximately $N_{ai} \approx 4 \times 10^{16} \text{ cm}^{-3}$. The extended layer following it is more strongly doped by an order of magnitude $N_a \approx 2 \times 10^{17} \text{ cm}^{-3}$. Without bias voltage, QWs are located in layer 1 in the SCR. Light doping at a contact potential of ~3.1 eV allows the creation of an SCR with a width of up to 300 nm, which is enough to accommodate up to five QWs.

To effectively use the QWs, it is desirable that the QWs are located at half-width of the SCR closest to the metallurgical boundary without bias voltage. The region doped more than the region where the QWs are located determines the contact potential.

Simulation of the modernized VCC was conducted using the MathCad package. The initial model parameters for the voltage–current characteristic model of a QW light-emitting diode are summarized in Table 1. The modeling parameters are adopted for the GNL-3014PGC light-emitting diode.

The experimentally obtained VCC is shown in Fig. 3 (solid curved line), on which are indicated (with circles) the coordinates of the calculated VCCs for structures with different numbers of QWs.

By selecting the coordinates and number of quantum wells, the width of the separation barriers, model dependences of the current through the p–n structure with the greatest coincidence of coordinates with the experimental VCC were obtained (Fig. 3). The optimum agreement was

obtained for a model structure with three quantum wells. The structure parameters were selected using the following method, which will be explained using a structure with three quantum wells. Current–voltage dependences of each quantum well were plotted using Eq. (16), as shown in Fig. 4. Model VCCs were constructed in the current range from 1×10^{-20} to 1×10^5 A without modeling the effect of their deviation from the exponent at high current densities. Two sections can be distinguished on them: (i) an exponential one, which is practically linear in semilogarithmic coordinates and (ii) a section described by a complex function caused by the competition of two exponentials in the denominator of Eq. (16). Moreover, the indicators of these exponentials depend on bias voltage owing to the dependence of SCR width on voltage.

In the exponential plot, the following is the denominator of Eq. (16):

$$\begin{aligned} & r \exp \left\{ \left(\frac{-\varphi_k + qU}{kT} \right) \left[\frac{2\mu}{W(U)} - \frac{\mu^2}{W(U)^2} \right] \right\} \gg \\ & \exp \left\{ (\varphi_k - qU) \left[1 - \left(\frac{2\mu}{W(U)} - \frac{\mu^2}{W(U)^2} \right) \right] \right\}. \end{aligned} \quad (18)$$

Therefore, the current depends on voltage according to the following law:

$$\begin{aligned} J_1(U) = J_{0QW} & \frac{\exp \left(\frac{-\varphi_k + qU}{kT} \right)}{r \exp \left\{ \left(\frac{-\varphi_k + qU}{kT} \right) \left[\frac{2\mu}{W(U)} - \frac{\mu^2}{W(U)^2} \right] \right\}} \\ & = \frac{J_{0QW}}{r} \exp \left[- \left(\frac{-\varphi_k + qU}{kT} \right) \left(1 - \frac{2\mu}{W(U)} + \frac{\mu^2}{W(U)^2} \right) \right]. \end{aligned} \quad (19)$$

In this case, the SCR edge is sufficiently far from the middle of the quantum well (Fig. 4(b)), satisfying the relation $W(U) > 2\mu$. The VCC derivative of a single QW in semilogarithmic coordinates is described by a relatively cumbersome equation. However, calculations in MathCad provide a graph of a linearly varying function, whose values range from 1 to 1.32 with variations in $\mu/W(U)$ from 0 to 0.5 during which current changes by 9 orders of magnitude.

Deviation from the exponent begins after the SCR's midpoint; i.e., the maximum recombination rate passes through the middle of the quantum well with further increase in forward bias voltage. In this case, the resulting dependence of current on voltage represents the coordinates of the points, so to speak, of the instantaneous values of the exponent with a variable indicator $\frac{2\mu}{W(U)} - \frac{\mu^2}{W(U)^2}$ and a changing ratio of the values of the denominator exponents in Eq. (16).

At a certain voltage, when the ratio of the exponents in the denominator in Eq. (16) changes as

$$\begin{aligned} & r \exp \left\{ \left(\frac{-\varphi_k + qU}{kT} \right) \left[\frac{2\mu}{W(U)} - \frac{\mu^2}{W(U)^2} \right] \right\} \ll \\ & \exp \left\{ (\varphi_k - qU) \left[1 - \left(\frac{2\mu}{W(U)} - \frac{\mu^2}{W(U)^2} \right) \right] \right\}, \end{aligned} \quad (20)$$

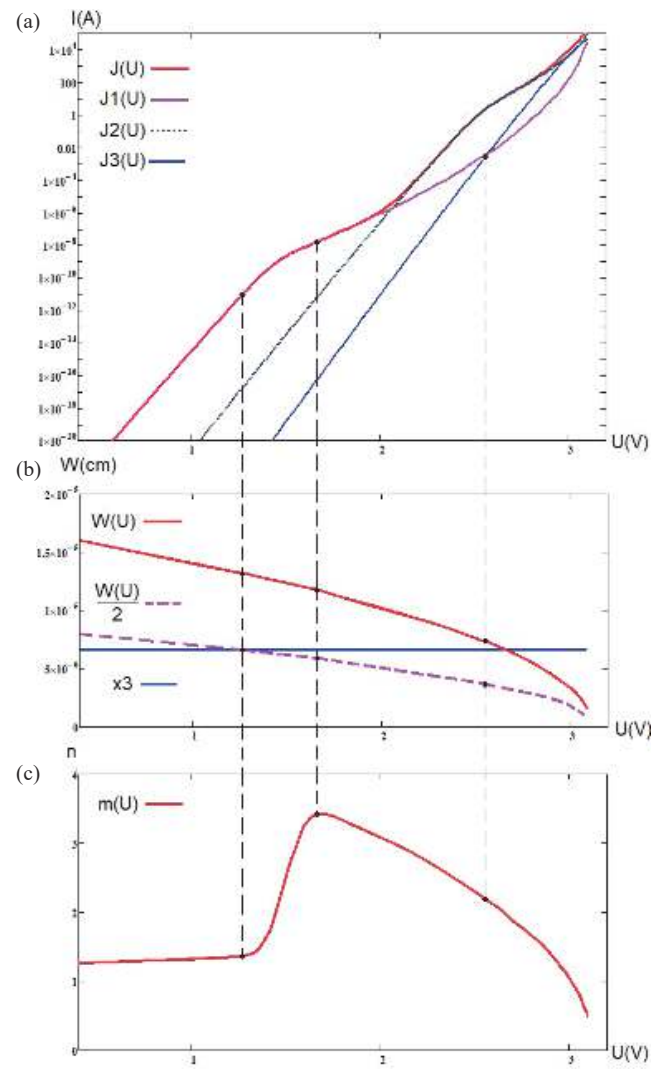


Fig. 4. (Colour online) Voltage–current characteristics of the quantum wells (a), VA is total VCC; numbers indicate the VCCs corresponding to location of quantum wells on the diagram of dependence of SCR edge and its middle (b), quantum wells are marked with black lines; (c) dependence of the VCC derivative in semilogarithmic coordinates of QW 3.

the derivative first reaches a maximum (Fig. 4(c), $(kT dU/d(\ln(J)) > 3$) and then decreases. When the quantum well shifts beyond the SCR, the derivative tends to the value 2 at $\mu/W(U) = 1$.

In this case, the dependence of current on voltage is expressed as

$$\begin{aligned} J_1(U) = J_{0QW} & \frac{\exp \left(\frac{-\varphi_k + qU}{kT} \right)}{r \exp \left\{ \left(\frac{-\varphi_k + qU}{kT} \right) \left[\left[1 - \left(\frac{2\mu}{W(U)} - \frac{\mu^2}{W(U)^2} \right) \right] \right\}} \\ & = \frac{J_{0QW}}{r} \exp \left[- \left(\frac{-\varphi_k + qU}{kT} \right) \left(\frac{2\mu}{W(U)} - \frac{\mu^2}{W(U)^2} \right) \right]. \end{aligned} \quad (21)$$

Fig. 5 shows a model diagram of VCC derivative dependence (on a semilogarithmic scale n) on bias voltage for the GNL-3014PGC LED structure with the parameters presented in Table 1.

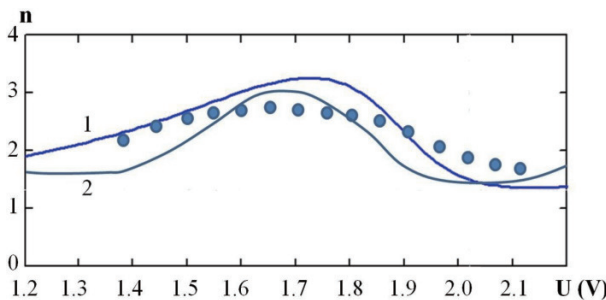


Fig. 5. (Colour online) Model dependences (on a semilogarithmic scale n) of VCC derivative on forward bias voltage, obtained using the parameters listed in Table 1 for a structure with (1) three QWs and (2) five QWs. The dots indicate the values of derivative of experimental VCC of the GNL-3014PGC LED structure.

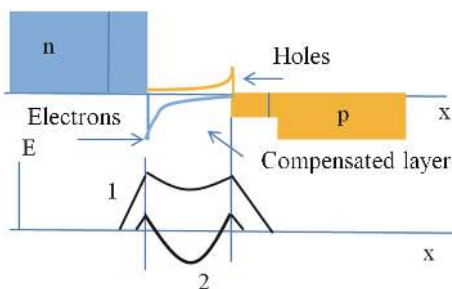


Fig. 6. (Colour online) Scheme of the formation of a built-in electric field of free charge carriers in a high-bandgap p-n homostructure: 1) diagram of the electric field in the SCR at low current densities up to 1 A/cm^2 ; 2) electric field diagram at high current densities $J > 1 \text{ A/cm}^2$: negative values indicate built-in field of free charge carriers creating voltage U_i .

A comparison of the simulation results for different numbers of QWs shows that the greatest agreement with the experimental VCCs and their derivatives was determined for a structure with three QWs.

Various researchers cite the following as a cause of the strong deviation of experimental VCCs from the one predicted via theory^[1, 2] at high current densities: (i) voltage drop across external contact resistances and (ii) thickness of the quasineutral part of the p and n regions. However, improvements in production technology of quantum well LEDs have not eliminated this effect.

Previous work^[24] showed that at the interface of p-n structures based on high-bandgap semiconductors with the same band gap in a lightly doped, compensated layer near the metallurgical boundary, under certain conditions, two regions of space charge can appear, namely, semiconductor ions and diffusing free charge carriers. Therefore, in a lightly doped layer of a p-n structure, a superposition of electric fields of stationary impurity ions and charges of diffusing charge carrier layers occurs. These fields have opposite directions. At low injection levels, the primary role in field distribution is played by the impurity ions in the SCR. When a relatively high injection level is attained, the diffusing charge carriers produce a sufficiently high opposite electric-field intensity, leading to a built-in voltage of the same polarity as the external bias voltage. Inside the SCR, a capacitor structure seems to originate from free charge carriers separated by a small spatial gap of a compensated semiconductor in the order of several hundred angstroms (Fig. 6). Calculations reveal that with a distance of

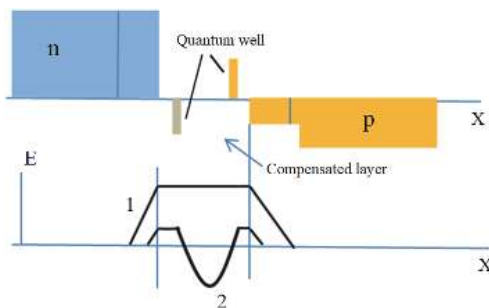


Fig. 7. (Colour online) Schematic of the formation of the built-in electric field of free charge carriers of QWs in a high-bandgap heterostructure: 1) diagram of the electric field in the SCR at low current densities up to 1 A/cm^2 ; 2) electric field diagram at high current densities $J > 1 \text{ A/cm}^2$: negative values indicate built-in field of free charge carriers creating voltage U_i .

$5 \times 10^{-6} \text{ cm}$ between the layers of free charge carriers and their excess concentration of $1 \times 10^{17} \text{ cm}^{-3}$, the electric-field intensity of the charge carriers will be $\sim 10^4 \text{ V/cm}$, which is close in magnitude to the field intensity of the impurity ions of the lightly doped layer but of the opposite sign. With increasing injection level, the field of free carriers inside the SCR becomes more notable and the total external bias voltage is equal to the sum of the potential barrier lowering voltage and the voltage produced by the field of free charge carriers $U = U + U_i$. Hereon, the VCC deviation from the exponential dependence starts. A previous study on VCCs^[25] can be an example of such a mechanism.

In light-emitting diode structures with QWs, a different mechanism can be implemented. As an example for its analysis, let us consider the model structure of the light-emitting diode in this study. In the injection mode, excess free charge carriers accumulate in QWs located in a relatively lightly doped active layer so that electrons and holes predominate on the side near the n-layer and p-layer, respectively (Fig. 7). Because these charge carriers produce a charge excess over the equilibrium one, the outermost QW can be represented as the capacitor coating with a charge $\pm\Delta Q$. The electric-field intensity vector of these charges is directed opposite to the SCR intensity vector of the p-n contact barrier.

With increasing injection level, the concentration of excess charge carriers in the QW increases, $\pm\Delta Q$ and the magnitude of the electric-field intensity produced by free carriers in QW increase, and the electric-field intensity of the barrier decreases. Above a certain injection level, the direction of the total voltage vector between the QW changes compared to the voltage vector of the potential barrier. Consequently, by further increasing the injection level, the total bias voltage at the terminals of the light-emitting diode structure is equal to $U = U_b + U_i$ and the VCC deviates from the exponential dependence. The beginning of the deviation corresponds to the equality of the electric-field intensities of the barrier SCR and the excess charge carriers in the QW. Calculations reveal that such a mode can occur at a current density of 1.0×10^{-1} – 1.0 A/cm^2 , i.e., with an excess concentration of charge carriers in QWs in the order of $\Delta n (\Delta p) = 1 \times 10^{16}$ – $1 \times 10^{17} \text{ cm}^{-3}$.

Based on high-bandgap GaN and AlInGaP semiconductors with practically similar design and technological parameters, it is clear that for light-emitting diode structures with QWs, this regime should be the same, which elucidates the

observed deviations of the VCCs from the exponential regime at the same high injection levels.

3. Conclusion

A physical and mathematical model of the voltage-current characteristics of light-emitting diode structures with QWs is designed based on a modernized model of the Sah–Noyce–Shockley recombination mechanism. In the modernized model, QWs are represented as radiative recombination centers discretely distributed in the SCR with a unit capture cross section. A distinctive feature of the presented model is that the probability of recombination rate in the SCR is described by a function whose value is 1 in the region of quantum wells and 0 in the region of separation barriers. This function complements the equation for the recombination rate according to the SNS model. Testing the model for different technological parameters of a structure with QWs demonstrates the possibility of obtaining the VCC derivative in semilogarithmic coordinates in the range of 1–4 only when considering recombination in the QWs, excluding tunneling and leakage currents. The improved model is compared with the experimental VCCs of specific samples using the experimental active region doping parameters obtained from the doping agent distribution profile.

Acknowledgments

The work was conducted within the state assignment of the Ministry of Science and Higher Education for universities (Project No. FZRR-2023-0009).

References

- [1] Shockley W. The theory of p-n junctions in semiconductors and p-n junction transistors. *Bell Syst Tech J*, 1949, **28**, 435
- [2] Sah C T, Noyce R N, Shockley W. Carrier generation and recombination in P-N junctions and P-N junction characteristics. *Proc IRE*, 1957, **45**, 1228
- [3] Moeini I, Ahmadpour M, Mosavi A, et al. Modeling the time-dependent characteristics of perovskite solar cells. *Sol Energy*, 2018, **170**, 969
- [4] Sabity M R, Ali G M. Staggered heterojunction Pentacene/ZnO based organic–inorganic flexible photodetector. *Results Opt*, 2023, **11**, 100403
- [5] Houshmand M, Zandi M H, Gorji N E. Degradation and device physics modeling of SWCNT/CdTe thin film photovoltaics. *Superlattices Microstruct*, 2015, **88**, 365
- [6] Moeini I, Ahmadpour M, Gorji N E. Modeling the instability behavior of thin film devices: Fermi Level pinning. *Superlattices Microstruct*, 2018, **117**, 399
- [7] Díaz S R. A generalized theoretical approach for solar cells fill factors by using Shockley diode model and Lambert W-function: A review comparing theory and experimental data. *Phys B Condens Matter*, 2022, **624**, 413427
- [8] Sze S M, Ng K K. Physics of semiconductor devices. New Jersey: John Wiley & Sons, 2007, 1, 1
- [9] Torchynska T V, Polupan G P, Kooshnirenko V I, et al. Mechanism of injection-enhanced defect transformation in LPE GaAs structures. *Phys B Condens Matter*, 1999, **273/274**, 1037
- [10] Manuel H, Iván L, Carlos A, et al. Improved GaInP/GaAs/GaInAs inverted metamorphic triple-junction solar cells by reduction of Zn diffusion in the top subcell. *Sol Energy Mater Sol Cells*, 2022, **248**, 112000
- [11] Manyakin F I, Vattana A B, Mokretsova L O. Application of the sah-noyce-shockley recombination mechanism to the model of the voltagecurrent relationship of led structures with quantum wells. *Light Eng*, 2020, 31
- [12] Grushko N S, Vostretsova L N, Ambrosevich A S, et al. Effect of temperature on luminance-current characteristics of the InGaN light-emitting diode's structure. *Semiconductors*, 2009, **43**, 1356
- [13] Masui H. Diode ideality factor in modern light-emitting diodes. *Semicond Sci Technol*, 2011, **26**, 075011
- [14] Masui H, Nakamura S, DenBaars S P. Technique to evaluate the diode ideality factor of light-emitting diodes. *Appl Phys Lett*, 2010, **96**, 073509
- [15] Pengchan W, Phetchakul T, Poyai A. The local generation and recombination lifetime based on forward diode characteristics diagnostics. *J Cryst Growth*, 2013, **362**, 300
- [16] de Vrijer T, van Nijen D, Parasramka H, et al. The fundamental operation mechanisms of nc-SiO_{x>0}:H based tunnel recombination junctions revealed. *Sol Energy Mater Sol Cells*, 2022, **236**, 111501.
- [17] Bulyarskii S V, Vorob'ev M O, Grushko N S, et al. Deep-level recombination spectroscopy in GaP light-emitting diodes. *Semiconductors*, 1999, **33**, 668
- [18] Özdemir O, Sel K. Study of minority carrier injection phenomenon on Schottky and plasma deposited p–n junction diodes. *Mater Sci Semicond Process*, 2009, **12**, 175
- [19] Manyakin F I, Mokretsova L O. The regularity of the decrease in the quantum yield of quantum-wells LEDs at the long-term current flow from the ABC model position. *Light Eng*, 2021, 62
- [20] Yu P Y, Cardona M. Fundamentals of semiconductors: Physics and materials properties. Berlin, Heidelberg: Springer Berlin Heidelberg, 2010, 1, 1
- [21] Adachi S. Handbook on physical properties of semiconductors. New York: Springer, 2004
- [22] Shockley W, Read W T. Statistics of the recombinations of holes and electrons. *Phys Rev*, 1952, **87**, 835
- [23] Kudryashov V E, Mamakin S S, Turkin A N, et al. Luminescence spectra and efficiency of GaN-based quantum-well heterostructure light emitting diodes: Current and voltage dependence. *Semiconductors*, 2001, **35**, 827
- [24] Manyakin F I. Mechanism and behavior of the light flux decrease in light-emitting diodes based on AlGaN/InGaN/GaN structures with quantum wells upon prolonged direct-current flow of various densities. *Semiconductors*, 2018, **52**, 359
- [25] Manyakin F I, Mokretsova L O. Modeling the energy structure of a GaN p–i–n junction. *Russ Microelectron*, 2018, **47**, 619



Fedor I. Manyakin, PhD, DSci in Physics and Mathematics. Professor, Leading Researcher of the Scientific and Technical Center "Optoelectronics" of Moscow Polytechnic University, Moscow, Russia. Author and co-author more than 160 publications. Research interests: semiconductor electronics, physics of semiconductor devices.



Dmitry O. Varlamov, Senior Lecturer of the Department of Electrical Equipment and Industrial Electronics of Moscow Polytechnic University, Moscow, Russia. Author and co-author of more than 40 publications. Research interests: microcontroller systems, LEDs.



Vladimir P. Krylov, PhD, DSci in Engineering. Professor of the Department of Biomedical and Electronic Means and Technologies, Head of the Scientific and Educational Center "CALS in Electronics" of Vladimir State University, Vladimir, Russia. His scientific interests are related to the physics of semiconductors and semiconductor devices, as well as to the issues of reliability of semiconductor electronic component base.



Arkady A. Skvortsov, PhD, DSci in Physics and Mathematics, Professor, Head of the Department of Mechanics of Materials, Moscow Polytechnic University, Moscow, Russia. Author and co-author of more than 150 articles and monographs on the study of semiconductor materials and problems of degradation of micro- and nanoelectronic systems.



Lyudmila O. Morketsova, Associate Professor at the Department of Computer-Aided Design and Engineering, National Research National University of Science and Technology "MISiS", Moscow, Russia. Research interests: three-dimensional modeling in lighting design.



Vladimir K. Nikolaev, Head of the Optoelectronics Science and Technology Center at Moscow Polytechnic University, Moscow, Russia. Author and co-author of more than 40 publications. Area of scientific interests: optoelectronics and instrumentation.